



Low-Cost and Active Control of Radiation of Wearable Medical Health Device for Wireless Body Area Network

Yong Jin¹

Received: 16 January 2019 / Accepted: 22 March 2019 / Published online: 8 April 2019
© Springer Science+Business Media, LLC, part of Springer Nature 2019

Abstract

Wearable devices, wireless networks and body area networks have become an effective way to solve the problem of human health monitoring and care. However, the radiation problems of wireless devices, the power supply problems of wearable devices and the deployment of body area networks have become obstacles to their wide application in the field of health care. In order to solve the above problems, this paper studies and designs a wearable health medical body area network which is convenient for human health monitoring and medical care, starting from low-cost deployment of wireless wearable devices and active control of wireless radiation. Firstly, in order to avoid replacing equipment batteries, improve the relay and data aggregation capabilities of wireless body area network, and reduce the communication and computing load of edge devices, a deployment scheme of wireless medical health wearable devices is designed based on the optimal segmentation algorithm of Steiner spanning tree. Then, in order to minimize the charging cost and maximize the global charging utility of single source and multiple points in a finite time slot, an approximate algorithm for the optimal charging sequence based on 01 knapsack problem, i.e., the access path of wireless wearable devices, is designed. Then, an active radiation control algorithm for wearable medical health body area network is proposed, which can actively control the transmission power and radiation status of these wireless devices. Finally, simulation results show that the proposed algorithm is better than battery-powered wireless body area network and wireless rechargeable body area network, 16% and 44% reduction of devices, 25% and 13% reduction of energy consumption, 26% reduction of radiation, and 5.18 and 1.13 times improvement of signal quality.

Keywords Cost optimization · Active control · Radiation · Wireless chargers · Wearable medical health care device · Wireless body area network

Introduction

With the development of topology control and networking technology of wireless body area network [1] [2], the hardware and software [3] of wearable devices have been widely used. However, wireless body area network nodes have obvious limitations [4] in power supply, computing power, communication capacity and so on. Especially, how to cooperate among complex [5] and heterogeneous wireless

wearable medical and health devices and how to reduce the system complexity [6] and computing power of wireless network are the key and difficult points in designing medical wireless body area network. At the same time, in order to improve the quality of user experience and the commercial competitiveness of wireless wearable devices and their networks, it is also the key to improve the medical wireless body area network to solve the energy support and prolong the network lifetime of wireless body area network.

At present, there are the following challenges in control and deployment of wearable medical health care body area network: (1) How to deploy the most suitable edge nodes and chargers. (2) How to control the radiation of wireless communication and schedule the edge nodes or chargers. (3) How to provide the quality of signal guarantee and network life cycle.

This article is part of the Topical Collection on *Mobile & Wireless Health*

✉ Yong Jin
jinyong@cslg.cn

¹ School of Computer Science & Engineering, Changshu Institute of Technology, Changshu 215500, China

in this paper, by enumerating all the communication paths of wireless body area network, we define a bottleneck Steiner tree problem and its approximate algorithm on the European plane, to deploy the least wireless charger, to improve the quality of user experience of medical health monitoring objects. Next, we design a global optimal access path, which can start from any single source point and find out the optimal charging sequence within a limited time slot, that is, the access sequence of other vertices, to minimize the charging cost and maximize the global charging utility. Then, we design an active radiation control algorithm for wearable medical and health body area network, which can actively control the transmission power and radiation status of these wireless devices.

The rest of the paper is organized as follows. In Section “[Related work](#)”, we give the related work. Section “[Deployment algorithm of wearable medical health device](#)” describes the deployment algorithm of wireless wearable medical health devices based on Steiner tree problem. In Section “[Low cost charging algorithms](#)”, we present the low-cost charging algorithms with dynamic Traveling Salesman Problem. Section “[Active controllable radiation algorithms for wearable medical health body area networks](#)” shows the active controllable radiation algorithms for wearable medical health body area networks. Section “[Experimental analysis and verification](#)” presents the simulation results, and concluding remarks are given in Section “[Conclusions](#)”.

Related work

About Wearable Body Area Network, Gao G P *et.al* proposed a wearable circular ring slot antenna with electromagnetic bandgap structure for wireless body area network application [7] and a new type of the wearable aperture-coupled patch antenna for 2.4 GHz wireless body area network (WBAN) application [8]. The authors of article [9] investigated the impact of introducing an additional substrate in order to improve the antenna performance, shielding effect in terms of SAR and degree of wear ability, in comparison with the standard topology. However, how to supply the power energy for the nodes of WBAN is lack of in-depth research.

About medical health care device, the article [10] researched the operational details of the instrument along with a brief review of the relevant literature. The authors of article [11] developed an air bio-battery for healthcare and medical applications, consisting of a glucose-driven enzymatic biofuel cell using a direct gas-permeable membrane or a gas/liquid porous diaphragm. The effective multi-step

approach was proposed in article [12] for the identification of a ‘purpose-specific active applicability window’ to maximize the antimicrobial activity of medical devices containing silver nanoparticles, minimizing any consequent risk for human health. However, how to manage and control the medical health care device and networking is still a problem.

About deployment of wireless chargers, in article [13], a hybrid optimization algorithm for energy storage management was proposed, which shifts its mode of operation between the deterministic and rule-based approaches depending on the electricity price band allocation. The proposed methodology by article [14] combined multiple sources of heterogeneous real-world data for the sake of deriving insights that can be of a great value to decision makers in the field. However, the above researches ignored the wireless charging cost in WBAN.

About radiation control, the authors of article [15] outlined the design of a piezoelectric line moment actuator used for active structural acoustic control. In article [16], the authors developed to model particle fluxes of secondary cosmic radiation in the Earth’s atmosphere, and calculated the characteristics of radio waves emitted by excess negative charge in an electromagnetic cascade. The article [17] provided a survey and tutorial of electromagnetic radiation exposure and reduction in mobile communication systems. However, how to active control the radiation in WBAN not only considering the wireless signal quality but also the radiation safety for Human is a key issue.

Deployment algorithm of wearable medical health device

With the wide application of Internet of Things, big data and cloud computing in medical, entertainment, military and industrial fields, people gradually pay attention to the application development and theoretical research of portable wireless devices and small-scale networks. Especially, with the reduction of production cost and the improvement of edge computing ability of various medical sensors, micro-cameras and portable medical devices, people have turned their attention to the research and development of wearable devices and their networks, such as personal area network, home care network, portable emergency network in public places and fast telemedicine vehicle network. Portable medical and health equipment with strong adaptability, high generalization and strong networking capabilities, the application of wireless body area network in medical monitoring, health care and remote first aid has been widely concerned. However, the above-mentioned medical

body area network has the following challenges to be solved urgently:

1. In wireless body area network, the power supply of the node is limited, and it is difficult to change batteries or wired charge these wearable devices because of the limited behavior of the monitored person.
2. The computing and communication abilities of the medical health monitoring edge devices mentioned above have obvious limitations. How to design the cooperation framework between the edge devices is the first problem to be solved.
3. In view of the limited energy and computational communication capability of the edge devices of wireless medical health monitoring, how to control the radiation of wireless devices to reduce the impact on the body of the monitored while extending the network lifetime as much as possible has become the key difficulty of wireless wearable medical health body area network.

In order to solve the energy shortage problem of health medical edge devices in wireless body area network, we will deploy a series of wireless chargers on the body and indoor environment, then form a charging network. The wireless charging network can avoid replacing batteries, and can be used as relay or sink nodes to reduce the communication and computing load of edge devices. Figure 1 shows a health care body area network application based on wireless charging network. Among them, several wireless chargers are deployed on the body of the monitored person, and several wireless chargers are deployed in the indoor environment. These chargers can charge edge devices and transmit medical health data.

In Fig. 1, suppose a monitored object deployed an independent self-organizing wireless body area network on each person. Each body area network deploys b wearable medical health edge devices (blue solid circle representation) and t wireless chargers (black solid rectangle representation). At the same time, j wireless chargers and c wireless base stations are deployed in the monitored environment.

The possible forwarding paths of medical monitoring data are as follows:

- Path 1, wearable edge device is sent to wireless charger, forwarded to base station and arrived at server.
- Path 2, the wearable edge device is sent to the base station to reach the server directly.
- Path 3, wearable edge devices are sent to the wireless charger in the environment, forwarded to the base station and arrived at the server.
- Path 4. Wearable edge devices are sent to wireless chargers, forwarded to wireless chargers in the environment, forwarded to base stations and arrived at servers.

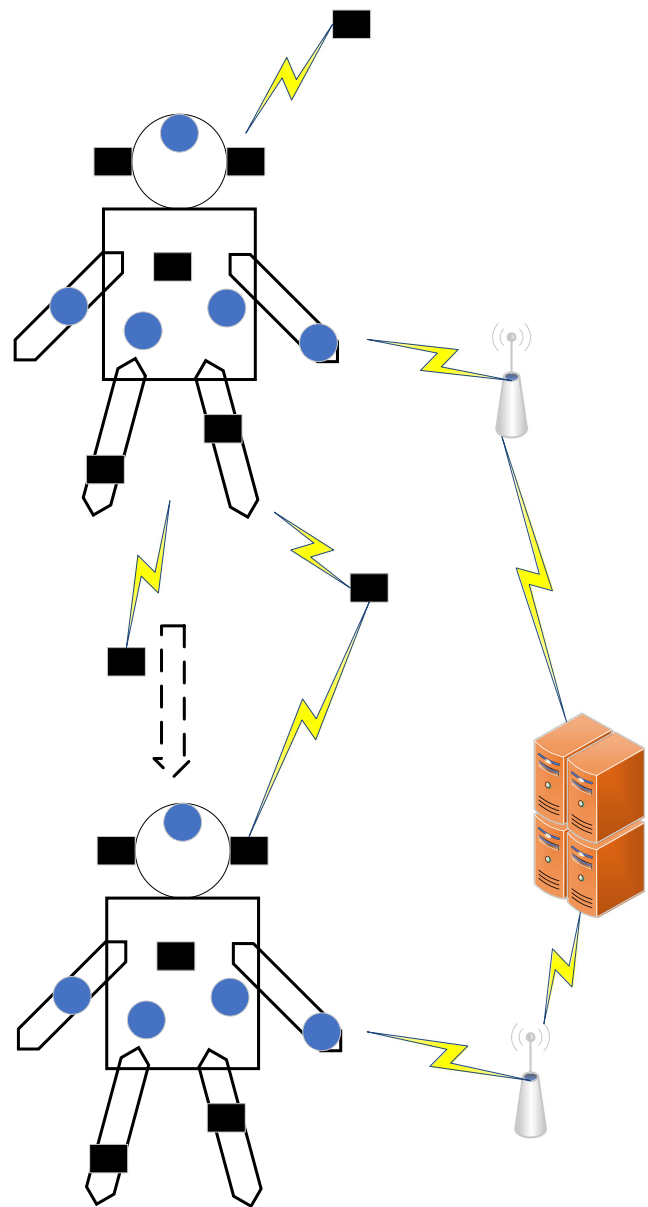


Fig. 1 Application of Wireless Charging-based WBAN

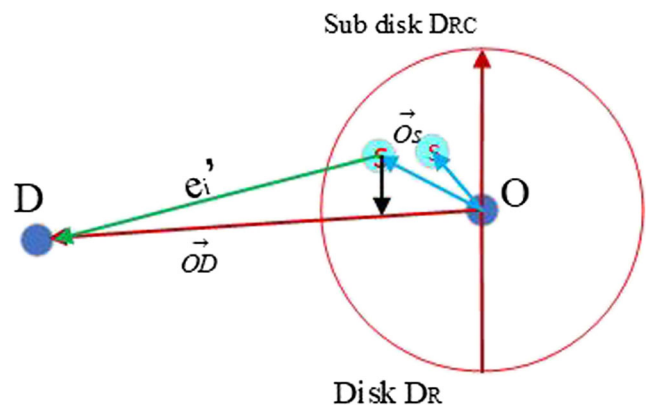


Fig. 2 edge segmentation

The difference between the above paths lies in the deployment and invocation of the internal wireless charger and the external wireless charger in the wireless body area network.

In order to improve the user experience quality of medical health monitoring objects, we define the above problem as a bottleneck Steiner tree problem on a European plane, and design an approximate algorithm to get an optimal solution.

On the body of the monitored person shown in Fig. 1, some edge devices for medical health monitoring have been deployed, defined as set P . It is hoped that by deploying k wireless chargers, the longest side of P set will be the shortest. The distance between any two points on set P is measured by Euclidean distance, and the value is greater than 0 and less than 2 m at the same time.

PIII.A (Deployment Problem of a Limited number of Chargers, DPLC) Given a set P and a positive integer k , a Steiner tree on P with at most k Steiner points is obtained to minimize the length of its longest edge.

We design an approximate algorithm with constant approximate ratio to solve PIII.A problem based on the optimal segmentation algorithm of Steiner spanning tree.

Algorithm III.A DPLC

input: $P, k > 0$

output: T

```

1 MST(P) ← invoking Algorithm III.B(P)
2 for each edge  $e \in \text{MST}(P)$ 
3    $N_s(e) \leftarrow 0$ 
4 end for
5 for  $i=1$  to  $k$  do
6   invoking Algorithm III.C
7    $N_s(e) \leftarrow N_s(e)+1$ 
8 end for
9 for each edge  $e \in \text{MST}(P)$ 
10   $e' \leftarrow$  average segmentation of edge  $e$  with  $N_s(e)$  Steiner Points
11   $T \leftarrow T \cup e'$ 
12 end for
13 return  $T$ 

```

Algorithm III.B SMT

input: P

output: $\text{MST}(P)$

```

1  $\text{MST}(P) \leftarrow$  invoking Prim algorithm
2 while  $P! = \emptyset$  do
3   deploy one point  $s$ ;
4   find a full component in  $P \cup s$ 
5    $\{max, p1\} \leftarrow \max\{\text{dis}(p, s) \mid \forall p \in P\}$ 
6    $\{s\_max, p2\} \leftarrow \max\{\text{dis}(p, s) \mid \forall p \in P \setminus p1\}$ 
7   if  $max \geq s\_max$ 
8      $PQ \leftarrow s \cup p1$ 
9   else
10     $PQ \leftarrow s \cup p2$ 
11  end if
12   $\text{MST}(P) \leftarrow \text{MST}(P) \cup PQ$ 
13 end while
14 return  $\text{MST}(P)$ 

```

Algorithm III.C Find the max value

input: e

output: rti

```

1 for each edge  $e \in \text{MST}(P)$ 
2   $Tem[i] \leftarrow$  ratio of length ( $e$ ) and  $N_s(e)$ 
3   $i++$ 
4 end for
5  $rti \leftarrow \max$  of  $Tem$ 
6 return  $rti$ 

```

Theorem III.A Algorithm III.A is the solution of DPLC with $(1 + \ln \gamma)$. Here, γ is the maximum length of OD.

Proof:

As shown in Fig. 2, define function $f(A) = |\overrightarrow{OA}|$, A is a selected Steiner point, representing the length of the cover on the vector $|\overrightarrow{OD}|$. $f(A_0) = 0$ means that the length of cover is 0 when no Steiner point is added. $f(A)$ is a submodular function.

$$f(A) + f(B) = f(A \cap B) + f(A \cup B).$$

Algorithm III.B chooses A_1, A_2, \dots, A_g , and put it in A. For each $i = 1, 2, \dots, g$. Denote $A_i = \{A_1, A_2, \dots, A_i\}$.

The minimum set of Steiner points means that the optimal solution is C_1, C_2, \dots, C_m , m is the number of Steiner points contained in the optimal solution of the minimum Steiner point problem.

According to algorithm III.B with greedy, A_{i+1} cover is not the longest vector $|\overrightarrow{OD}|$ part of A_i cover. U_i is a sub vector in a vector $|\overrightarrow{OD}|$ that is not covered, then $|U_i| = |\overrightarrow{OD}| - f(A_i)$.

Because U_i can be divided by m Steiner points, according to the pigeonhole principle, there must be a Steiner point C_j is at least $\frac{|\overrightarrow{OD}| - f(A_i)}{m}$ length covered by the $|\overrightarrow{A_i C_j}|$ of U_i .

Then,

$$\begin{aligned} f(A_{i+1}) - f(A_i) &\geq \frac{|\overrightarrow{OD}| - f(A_i)}{m} \\ \Rightarrow f(A_{i+1}) &\geq f(A_i) + \frac{|\overrightarrow{OD}| - f(A_i)}{m} \\ \Rightarrow -f(A_{i+1}) &\leq -f(A_i) - \frac{|\overrightarrow{OD}| - f(A_i)}{m} \\ \Rightarrow |\overrightarrow{OD}| - f(A_{i+1}) &\leq |\overrightarrow{OD}| - f(A_i) - \frac{|\overrightarrow{OD}| - f(A_i)}{m} \\ \Rightarrow |\overrightarrow{OD}| - f(A_{i+1}) &\leq \left(|\overrightarrow{OD}| - f(A_i) \right) \left(1 - \frac{1}{m} \right) \end{aligned}$$

After $i + 1$ recursive iteration, we get that,

$$\Rightarrow |\overrightarrow{OD}| - f(A_{i+1}) \leq |\overrightarrow{OD}| \left(1 - \frac{1}{m} \right)^{i+1}$$

because, $|U_i| = |\overrightarrow{OD}| - f(A_i)$,

$$|U_i| = |\overrightarrow{OD}| - f(A_i) \leq |\overrightarrow{OD}| \left(1 - \frac{1}{m} \right)^i \leq |\overrightarrow{OD}| e^{-\frac{i}{m}}$$

In addition, the length of U_i coverage decreases from $|\overrightarrow{OD}|$ to 0, so there must be a positive integer $i \leq g$ for $|U_{i+1}| < m \leq |U_i|$.

When algorithm III.B iterates to $i + 1$, only $m - 1$ elements are left uncovered at most. Therefore, after another iteration of

$m - 1$, greedy algorithm III.B will terminate, that is, there is $g \leq i + m$. In addition, $m \leq |U_i| \leq |\overrightarrow{OD}| e^{-\frac{i}{m}}$, so $i \leq m \cdot \ln \frac{|\overrightarrow{OD}|}{m}$. Here, $\gamma = \frac{|\overrightarrow{OD}|}{m}$, so $i \leq m \cdot \ln \gamma$ and $g \leq i + m \leq m + m \ln \gamma = m(1 + \ln \gamma)$, namely, $\frac{g}{m} \leq (1 + \ln \gamma)$.

Theorem III.A Proved.

The above algorithm solves the problem of wireless charger deployment on the monitored person. An improved algorithm III.A is presented below to solve the problem of wireless charger deployment in the monitored person's active environment.

ST is defined as the set of all possible states of the environment, X is the set of all perceived data of the monitored person, A is the set of all possible behaviors of the monitored person.

Thus, the monitored person can be described by a triple tuple $MP = \langle I, TR, PU \rangle$. Here, $I: S \rightarrow X \times A$, expressing the Integration of Environmental State and Behavior. $TR: S \rightarrow Z+$, denoting the wireless channel Quality of environment. $PU \leftarrow S \times A$, representing the deployment status of wireless chargers in the environment.

The path measurement of Algorithm III.A is changed to signal strength and normalized by formula (1).

$$\begin{cases} R(x) = \sum_{i=1}^a \gamma x_i \\ V(x) = \lim_{j \rightarrow \infty} \left(\frac{R(x)}{(b + t)^j |X|} \right) \end{cases} \quad (1)$$

Low cost charging algorithms

The algorithms in section “Deployment algorithm of wearable medical health device” implement the deployment of wireless chargers in the monitored person and the surrounding environment. The deployment scheme not only realizes charging the edge equipment of medical health monitoring, but also acts as a relay and forwarding node in real time. However, how to achieve wireless charging at the lowest cost within a limited range of charging capacity has not yet been solved.

The wireless body area network shown in Fig. 1 is defined as the complete graph $G = (V, E, C)$. Vertex set V includes edge device set ED, body charger set BC, and active environment charger set EC, namely $P = (ED, BC, EC)$. Edge set $E = e(i, j)$, where i denotes the starting point of E and j denotes the end point of E. Cost function C is used to calculate the cost of one charge. For function C, we give the following description.

- $\forall e(i, j) \in E_{BC}$ and if $i, j \in BC$, then $C(e) = 0$; where E_{BC} means that both ends of the edge are the edge sets of chargers inside the wireless body area network. The

charging cost of internal charger in wireless body area network is 0.

- (2) $\forall e \in E - E_{EC}$ and preserving the vertices of E_{BC} . Then, $C(e) > 0$. Here, $C_{data}(e) = \frac{dist(e)}{SI_{BC}}$. SI_{BC} is the signal intensity of the charger per unit distance. $C_{data}(e)$ represents the cost of charging data collection. $C_{charging} = T_{charging} BC_R$. BC_R is the working energy consumption of the charger per unit time. Charging time of edge devices obeys normal distribution with mean value of 0 and variance of 1, namely, $t(ED) = \frac{1}{\sqrt{2\pi}} e^{-\frac{ED^2}{2}}$.

The problem of charging cost minimization can be formalized as follows.

- Solution: $x_e, e \in E, \{0, 1\}$.
- Object: $\min \sum_{e \in E} C(e)x_e, e \in E, x_e \in \{0, 1\}$.

Additionally, the following constraints must be met:

- (1) All edge devices are accessed, i.e., $\{e \in E | x_e = 1\} \cap \{v(E_S)\} = E$. That is to ensure that each edge device is charged.
- (2) The working energy of the wireless body area network does not exceed the charging capacity constraint of the charger, i.e., $\sum_{e \in E} C(e)x_e \leq (E_{BC}^{max} + E_{EC}^{max}) \sum_{e \in BC \cup EC} x_e$. The total energy consumption of charging all edge devices does not exceed the total energy consumption of the charger in the wireless body area network and the charger deployed in the surrounding environment.
- (3) Real-time constraints on charging, i.e., $T_{ED}^{total} + T_{BC}^{total} + T_{EC}^{total} \leq \frac{E_{init}}{ED_W}$. Here, E_{init} indicates the initial energy of each edge device and ED_W denotes the unit time energy consumption of the edge device. And, $\forall i, j \in ED, E_{init}(i) = E_{init}(j)$.
- (4) Uniqueness of Charging Object of Charger. The charger should be divided into a closed loop as a unit, and divided into k unwanted loops, that is, the BC contains k independent charging loops, such as BC_1, \dots, BC_k . Among them, $\forall e(i, j) \in E_{BS}^l, i, j \in E_{BC}^l, j = (i + 1) \bmod |BC_l|, l = 1, 2, \dots, k$. And, $\sum_{m=1}^k \sum_{q=1}^{|BC_m|} |BC_m^q| = 1$ denotes the charger numbered q belongs to and only belongs to a closed loop.

Therefore, the problem of charging cost minimization is defined as follows:

PIV.A Visit each vertex within a specified time T_L and charge it; design access paths to minimize global charging costs and maximize charging utility. Starting from single source point

P_1 , in m slots, the optimal charging order, i.e. the access order of other vertices, is solved to minimize the charging cost and maximize the global charging utility.

The charger will traverse the updated collection $\bar{P} = \{P_1, P_2, \dots, P_n\}$ in the order of accessing it.

$$\text{charging utility max. } \sum_{i=1}^n U_i = \max. \sum_{i=1}^n \sum_{\substack{j=2 \\ i \neq j}}^n \frac{T_{charging}^{P_i}}{C_{i,j}}$$

Notice that, parameter $E_{RE}^{t_j, P_i}$ denote that vary with each time slot. $T_{charging}^{P_i} = \frac{E_{init} - E_{RE}^{t_j, P_i}}{U_{node}}$. $T_{dead} = \frac{E_{init}}{U_W}$. The time is discretized. Unit time slot is denoted as T_{slot} . timeslot number is $m = \frac{T_{dead}}{T_{slot}}$. Vertex number is $n = |V|$. The path distance between any two vertices is known and uniquely denoted as $C_{i,j} \triangleq T_{slot}^{i,j} = \frac{d(i,j)}{SI_{BC}} + \sum_{V_k \in V^{i,j}} T_{BC}^{V_k} + \sum_{V_k \in V^{i,j}} T_{EC}^{V_k}$. Where d(i, j) denotes the actual distance between vertex i and vertex j.

The above optimization problems need to satisfy the following constraints:

- (1) The number of slots allocated to each edge device $ED_{slot}^{charging,i} \geq \frac{T_{charging,j}}{T_{slot}} \cdot \frac{T_{charging,i}}{T_{slot}} = \left\lceil \frac{T_{charging}^{P_i}}{T_{slot}} \right\rceil$ is the number of time slots required for the first edge device to be fully charged. $T_{charging}^{P_i} = \frac{E_{init} - E_{RE}^{t_j, P_i}}{ED_W}$, $E_{RE}^{t_j, P_i}$ represents the remaining energy of the P_i vertex in the t_j slot.
- (2) $\sum_{i=1}^n ED_{slot}^{charging,i} \leq m$. The complete solution to the above problem and its classification are recorded as D_{tsp} described as follows:
 - (a) The TSP approximation Algorithm IV.A uses greedy algorithm on graph G and obtains the optimal path. We set a TSP threshold T_{TSP} . the parameter of T_L denotes the life cycle of the emotional device.
 - (b) If $T_L = T_{TSP}$ it indicates that the charger can only use TSP path.
 - (c) If $T_L > T_{TSP}$ the life cycle of rechargeable equipment is enough and the charging efficiency of TSP path is low. At this time, the 01-knapsack problem is adopted to maximize the charging utility.
 - (d) $T_L < T_{TSP}$ shows that the current state charger cannot access all chargeable devices within the time constraints. The 01-knapsack problem can be used to maximize charging effectiveness. The whole Steiner tree is segmented.

The solution to the problem is described as follows:

Firstly, the scale of TSP accessing edge devices is reduced, and the tree corresponding to graph G is divided

into $\left\lceil \frac{T_L}{T_{TSP}} \right\rceil$ sub-trees, then $D_{_tsp}$ is called. The time of subtree of $1, 2, \dots, \left\lceil \frac{T_L}{T_{TSP}} \right\rceil - 1$ are T_{TSP} . The time of subtree $\left\lceil \frac{T_L}{T_{TSP}} \right\rceil$ is $\text{mod} \left(\frac{T_L}{T_{TSP}} \right)$. Thus, TSP solution algorithm of greedy would be executed on subtree $1, 2, \dots, \left\lceil \frac{T_L}{T_{TSP}} \right\rceil - 1$. Algorithm IV.B for 01 knapsack problem aiming at maximizing charging utility would be invoked on subtree $\left\lceil \frac{T_L}{T_{TSP}} \right\rceil$.

Algorithm IV.A TSP with greedy

```

1 V[1]←1
2 temp←0
3 for i=1 to size of V do
4 D[i, i] ←0
5 end for
6 j← min{d(i, j), i, j∈size of V}
7 while i<=size of V do
8 temp←temp+D[0, j]
9 if i<=V/2 do
10 temp←temp+D[i, j]
11 end if
12 end while
13 return temp
    
```

Algorithm IV.B 01-knapsack with greedy

```

1 invoking Algorithm IV.A
2 for i = 0 to size of temp do
3 order the temp[i] with ascending order of ratio of  $C_{i,i+1}$ 
4 end for
5 if  $\sum temp < m$  do
6 return temp
7 else
8 return  $temp_k \leftarrow \max \left\{ temp_k, \sum_{i=1}^k temp_i \right\}$ 
    
```

Theorem IV.A As the solution of 01-knapsack problem, the approximation ration of Algorithm IV.B with greedy is smaller than 2.

Proof:

Let opt denote the objective function value of the optimal solution, and C_G is the objective function value of the approximate solution generated by algorithm 2.C, then the approximate ratio does not exceed 2, that is $opt \leq 2C_G$.

Assuming that $\sum_{i=1}^n c_i = C$, then $C_G = opt$. A knapsack can pack everything.

Suppose $\sum_{i=1}^n c_i > C$, j is an integer obtained by algorithm 2.C. The following inequalities can be obtained, $\sum_{i=1}^j c_i \leq opt$.

The maximum value $\hat{c} \geq opt$ of linear programming can be obtained by replacing $x_i = 0$ or 1 with $0 < x_i < 1$,

$$x_k = \begin{cases} 1, k = 1, 2, \dots, j \\ \frac{C - \sum_{i=1}^j c_i}{c_{j+1}}, k = j + 1 \\ 0, k = j + 2, j + 3, \dots, n \end{cases}, \quad opt \leq \hat{c} = \sum_{i=1}^j c_i + \frac{v_{j+1}}{c_{j+1}}$$

$$\left(C - \sum_{i=1}^j c_i \right) < \sum_{i=1}^j c_i + \frac{v_{j+1}}{c_{j+1}} c_{j+1} = \sum_{i=1}^{j+1} c_i. \text{ So, } \sum_{i=1}^j c_i \leq opt < \sum_{i=1}^{j+1} c_i$$

$$c_i \text{ and } C_G = \max \left\{ c_{j+1}, \sum_{i=1}^j c_i \right\} \geq \frac{1}{2} \sum_{i=1}^{j+1} c_i > \frac{1}{2} opt, \text{ namely, } \frac{opt}{C_G} \leq 2.$$

Theorem IV.A Proved.

Active controllable radiation algorithms for wearable medical health body area networks

Wireless communication devices such as wearable edge devices, chargers and chargers deployed in the surrounding environment, which are deployed on the monitored person’s body, will produce certain radiation. If not controlled, it will affect human health. Therefore, how to actively control the transmission power and radiation status of these wireless devices has become a key technology.

Based on the triple description of the monitored person in section “Deployment algorithm of wearable medical health device”, the following is redefined:

1. Described by tuple $\langle I, TR, PU, T \rangle$.
2. $I: S \leftarrow X * BC$, which represents the fusion of radiation state and charging behavior of edge devices.
3. $TR: S \leftarrow Z^+$, indicating the radiation status of wireless chargers deployed in the environment



4. $PU \leftarrow (S,A)*S'$, where $S' \subseteq S$ represents the radiation status of an independent wireless body area network.
5. $T: t \leftarrow f(x,t)*S'$, which indicates the radiation state transition.

The radiation state value function $RD(v, t)$ has the properties shown in formula (2). These three forms are defined according to the transmission power of wireless devices.

$$\begin{cases} RD(t) = \sum_{t=0}^{\infty} PU_t \\ RD(x, t) = \frac{\sqrt{|T|}}{\sum_{i=1}^{|X|} f(x, t)} \\ RD(t) = \lim_{t \rightarrow \infty} \left(\frac{TS \cdot PU}{|X|} \right) \end{cases} \quad (2)$$

We design an active strategy to minimize radiation while meeting the requirements of section “3 and 4”. We use the inverse method to obtain the desired active radiation control strategy. If the feasible active controllable strategy is η , the value of S in the radiation state is,

$$RD_S^\eta(t) = \sum_{t=0}^T \eta(V, t) \sum_{S'} RD(x, t) \quad (3)$$

Formula (3) can ensure that the radiation value obtained by adopting strategy η does not exceed the threshold value.

The radiation master function $SC(\eta, t)$ denotes the expected radiation value of the radiation state S after the execution of the master control behavior when the strategy η is adopted.

$$SC(\eta, t) = E_\eta \left\{ \sum_{t=0}^T V(x, t) \|R(x)\| > 0, x \in S' \right\} \quad (4)$$

When implementing strategy η , the same radiation state value may occur many times. The update of radiation state value in each iteration can be used as prior knowledge for active control in the next iteration, such as formula (5).

$$\eta_{t-k}(s) = \max \left\{ X | V^{\eta_{t-1}}(s') \sum_{S'} RD_{S'}^t \right\} \quad (5)$$

Using formulas (6) and (7) to update the radiation state value in strategy η will help to optimize the transmission power of wireless edge devices.

$$TR^{\eta_t}(s) = \frac{\sum \eta_{t-k} \cdot f(s, t)}{|I_{S'}^t| \sum_{S'} RD_{S'}^t} \quad (6)$$

$$SC_{t-k}(\eta_t, T) = \frac{\sum_{t=0}^{\infty} PU_t}{\max_{S'} TR^{\eta_t}(s)} \quad (7)$$

The process flow of heuristic algorithm used to implement the above process is shown in Fig. 3, and the code is described as follows:

Algorithm V.A Active Control Radiation

- 1 For each charging time
- 2 For each edge devices in V
- 3 For each radiation state S
- 4 executing formula (2) based on the transmitting power
- 5 Get the radiation value
- 6 End for
- 7 update the radiation value based on formula (3)
- 8 End for
- 9 active control the radiation value based on formula (6) and (7)
- 10 End for

Experimental analysis and verification

Based on the wireless body area network model shown in Fig. 1, the nodes have been deployed as shown in Fig. 4. The location of the wireless sensor node is completely referred to in Fig. 4. Here, it is assumed that all sensor nodes have the same battery capacity and can be charged wirelessly. In the simulation, the trajectory of the experimenter obeys Poisson distribution, and the change of body posture obeys Markov chain model. In the experiment, only static, walking and

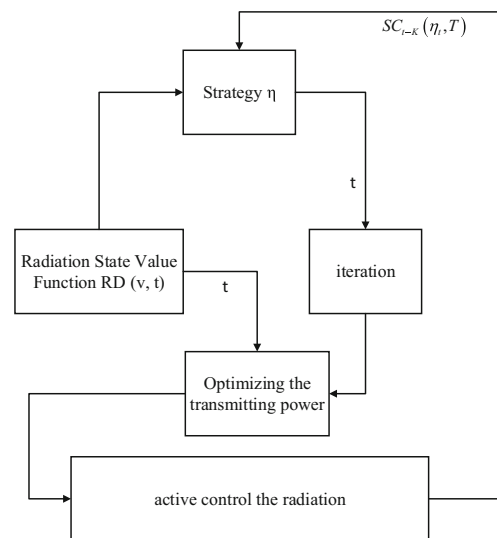
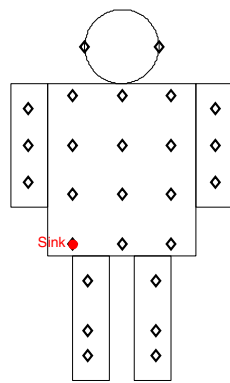
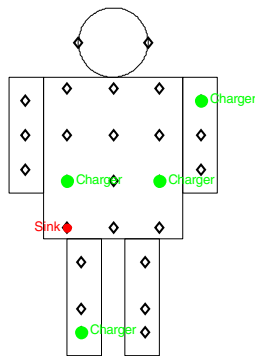


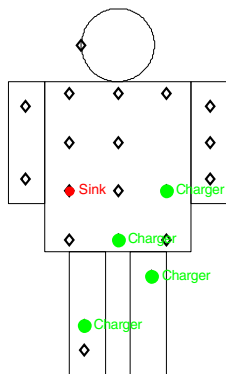
Fig. 3 active control algorithm the radiation



(a) WBAN-batteryAlone



(b) WBAN-chargingAlone



(c) WBAN-proposedAlgs

Fig. 4 Node deployment topology

jogging were considered, and their steady-state probabilities were set to 0.2, 0.35 and 0.45, respectively. The simulation parameters are shown in Table 1.

In the experiments, we defined the following three schemes,

- (1) *WBAN-batteryAlone* indicates that a wireless body area network node consists of an energy-constrained battery-powered node and a sink node.

Table 1 simulation parameters

Parameter	Value
bandwidth	2 MHz
Wireless transmission rate	[121, 486] kbps
Energy Consumption in Wireless Transmission	0.65uw
Node number	20
Number of personnel	6

- (2) *WBAN-chargingAlone* indicates that wireless body area network nodes are composed of energy-constrained battery-powered nodes, some chargers and a sink node.
- (3) The wireless body area network represented by *WBAN-proposedAlgs* consists of path and communication optimized edge nodes, wireless chargers and sink nodes.

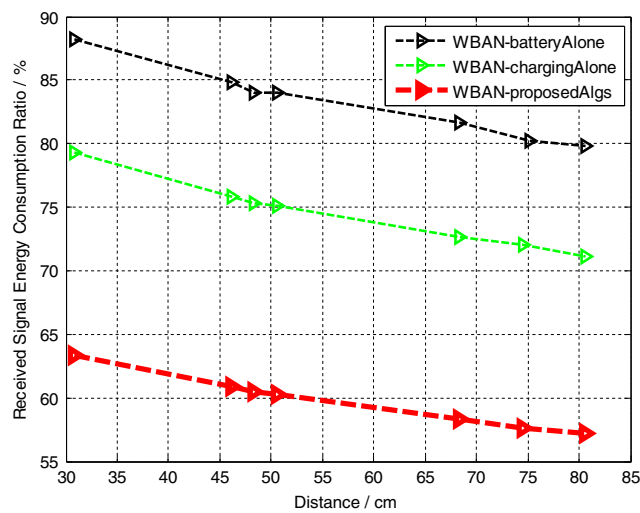
Based on the code of Chapter 14 in Ref [18], titled with “Q-learning-based routing method for wireless body area networks”, we implemented the above three algorithms using MATLAB and C++ and verified them by statistics of Network Topology, Energy Consumption, Radiation Intensity and Signal Quality, etc.

Figure 4 shows the network topologies of *WBAN-battery Alone*, *WBAN-charging Alone* and *WBAN-proposedAlgs* respectively. Analyzing Fig. 4, *WBAN-battery Alone* deploys 25 energy-constrained battery-powered nodes, one sink node. *WBAN-chargingAlone* deployed 21 energy-constrained battery-powered nodes, four wireless chargers and one sink node, which reduced the number of health monitoring nodes by 16%. *WBAN-proposedAlgs* deployed 14 edge nodes, 4 wireless chargers and 1 sink node after path planning and communication optimization. Compared with *WBAN-battery Alone*, the medical health monitoring node decreased by 44%.

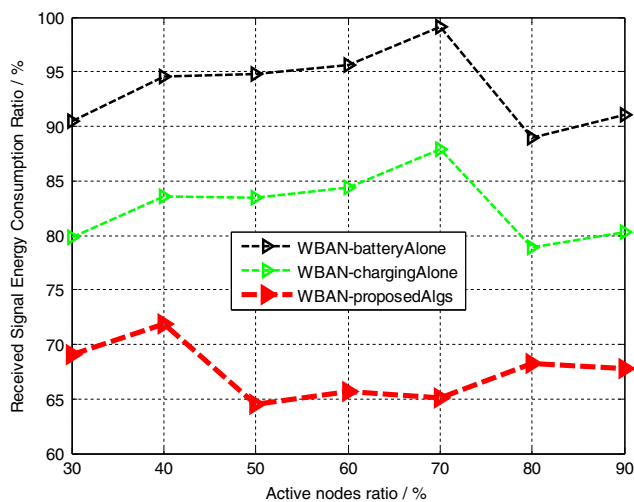
Figure 5 shows the energy consumption ratios of sink nodes in three schemes based on distance and active edge node rate. Figure 5a shows that with the increase of communication distance between edge nodes and sink nodes, the energy consumption ratio decreases gradually. This is because cooperative communication and relay forwarding between edge nodes can help to reduce the received signal energy of sink nodes over long distances. However, the performance of *WBAN-batteryAlone* scheme is the worst, because the energy of edge nodes is limited and can not pay too much energy for the ultimate forwarding, thus not participating in or less participating in end-to-end cooperative communication. *WBAN-chargingAlone* scheme deploys some wireless chargers, so relay nodes actively participate in relay forwarding, and wireless chargers can be used as auxiliary nodes of sink nodes, thus effectively reducing the energy of sink nodes to receive signals. However, the deployment density of edge nodes and wireless chargers in *WBAN-chargingAlone* scheme is relatively high, and the signal radiation between them will seriously

reduce the received signal quality of sink nodes. To avoid this problem, the cooperative communication contribution of wireless chargers will inevitably decrease with the increase of the cooperative proportion of edge nodes, so the received signal energy consumption of sink nodes in this scheme is only lower. It dropped by 10%. In contrast, *WBAN-proposedAlgs* solves the problems of the above two schemes well, and the received signal of sink node can save 28% energy. Figure 5b shows the performance of the three schemes with the increase of active edge nodes. The *WBAN-proposedAlgs* scheme saves 25% and 13% energy compared with the *WBAN-battery Alone* scheme and the *WBAN-charging Alone* scheme, respectively.

The abscissa of Fig. 6 shows the distance between the transmitter and the receiver of the wireless monitoring signal. Longitudinal coordinates represent the radiation intensity of the wireless communication process. From Fig. 6, we can see



(a) with distance



(b) with active nodes ratio

Fig. 5 Sink Point Received Signal Energy Consumption Ratio

that *WBAN-batteryAlone* scheme is more than 40 $\mu\text{W}/\text{cm}^2$ in order to improve the transmission quality and robustness of wireless monitoring signals, and it is very likely to cause harm to human body. The radiation intensity of *WBAN-proposedAlgs* scheme and *WBAN-charging Alone* scheme is within the acceptable range, but the radiation intensity of *WBAN-proposedAlgs* scheme is 26% lower than that of *WBAN-chargingAlone* scheme.

Figure 7 illustrates the life cycle support capabilities of the three schemes. It can be seen that the wireless signal quality of *WBAN-batteryAlone* scheme increases slowly with the increase of active nodes. It should be noted that the network lifecycle analyzed in Fig. 7 considers not only the topological integrity of the network, but also the transmission quality of the wireless medical health monitoring signal. *WBAN-chargingAlone* scheme has been greatly improved in network life cycle and signal quality due to its rechargeability and multiple sink auxiliary nodes. However, the available signals of *WBAN-proposedAlgs* scheme are 5.18 times and 1.13 times higher than those of *WBAN-batteryAlone* scheme and *WBAN-charging Alone* scheme, respectively.

Conclusions

In order to reduce the communication and computing load of wearable devices, improve the efficiency of wireless network execution and the lifecycle of body area network, and combine the application requirements of human health monitoring and care with the actual deployment environment, this paper studies a series of algorithms and schemes of low-cost power supply for radiation controllable and wearable devices in wireless body area network. Our main contributions include: (1) By deploying some wireless chargers as relay nodes and data aggregation roles in wireless body area networks, an

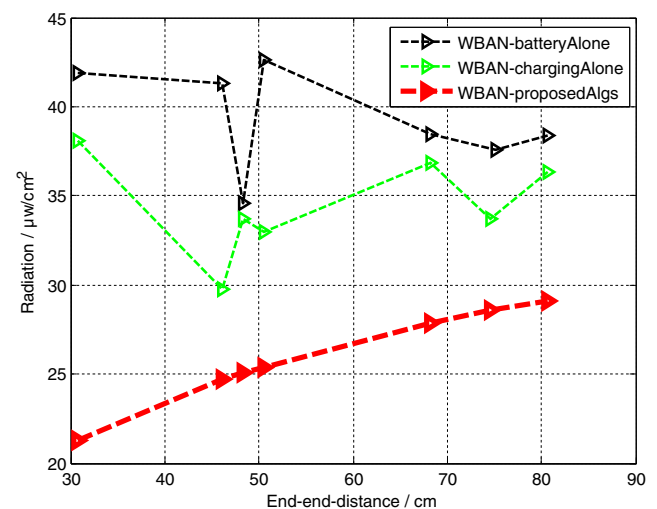


Fig. 6 Radiation

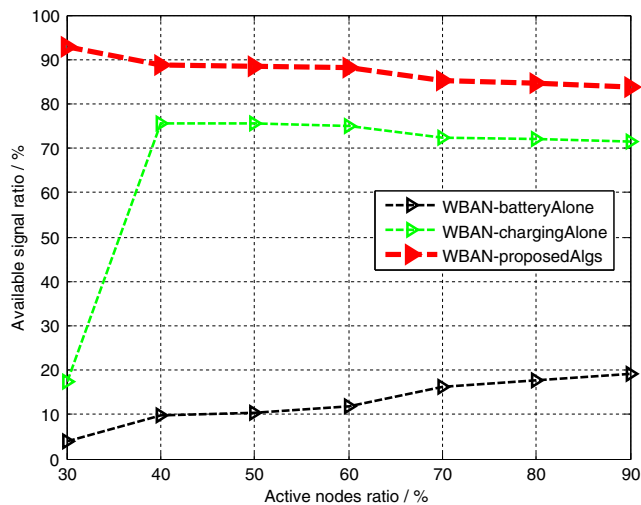


Fig. 7 Signal quality with active nodes ratio

approximate algorithm and its deployment scheme for wireless health wearable devices are designed based on the optimal segmentation algorithm of Steiner spanning tree, which can effectively reduce the communication and computing load of emotional edge devices. (2) Based on the single-source multi-point path planning and time constraints, an approximate algorithm for the optimal access path of wireless wearable devices is designed to minimize the charging cost and maximize the global charging utility. (3) On the basis of reducing deployment cost and providing energy support, an active radiation control algorithm for wearable medical and health body area network is designed to actively control the transmission power and radiation status of wireless devices. Based on the deployment of wireless wearable devices, energy consumption of data collection, radiation intensity and signal quality, the simulation experiments compare and analyze battery-powered wireless body area network, wireless rechargeable body area network and radiation-controlled wireless rechargeable medical and health body area network. The results show that the proposed algorithm and its scheme are effective, such as 16% and 44% reduction of devices, 25% and 13% reduction of energy consumption, 26% reduction of radiation, and 5.18 and 1.13 times improvement of signal quality.

Acknowledgements The authors would like to thank the support from the Jiangsu Students' innovation and entrepreneurship training program (NO.201810333029Y).

Compliance with ethical standards

Conflict of interest We declare that we have no conflict of interest.

Human and animal rights This article does not contain any studies with human participants or animals performed by any of the authors.

Informed consent Informed consent was obtained from all individual participants included in the study.

References

1. Latré, B., Braem, B., Moerman, I. et al., A survey on wireless body area networks. *Wirel. Netw* 17(1):1–18, 2011.
2. Jain, P. C., *Wireless Body Area Network for Medical Healthcare*. IETE Tech. Rev. 28(4):362–371, 2011.
3. Ben Elhadj, H., Chaari, L., and Kamoun, L., A Survey of Routing Protocols in Wireless Body Area Networks for Healthcare Applications. *International Journal of E-Health and Medical Communications (IJEHMC)* 3(2):1–18, 2012.
4. Rathee, D., Rangi, S., Chakarvarti, S. K. et al., Recent trends in Wireless Body Area Network (WBAN) research and cognition based adaptive WBAN architecture for healthcare. *Heal. Technol.* 4(3):239–244, 2014.
5. Tahir, S., Bakhsh, S. T., Alghamdi, R. et al., Fog-Based Healthcare Architecture for Wearable Body Area Network. *Journal of Medical Imaging & Health Informatics* 7(6):1409–1418, 2017.
6. Varga, N., Piri, E., and Bokor, L., Network-assisted Smart Access Point Selection for Pervasive Real-time mHealth Applications. *Procedia Computer Science* 63:317–324, 2015.
7. Gao, G. P., Hu, B., Wang, S. F. et al., Wearable Circular Ring Slot Antenna With EBG Structure for Wireless Body Area Network. *IEEE Antennas & Wireless Propagation Letters* 17(3):434–437, 2018.
8. Gao, G., Hu, B., Tian, X. et al., Experimental study of a wearable aperture-coupled patch antenna for wireless body area network. *Microw. Opt. Technol. Lett.* 59(4):761–766, 2017.
9. Gil, I., and Fernándezgarcía, R., Wearable PIFA antenna implemented on jean substrate for wireless body area network. *Journal of Electromagnetic Waves & Applications* 31(11-12):1–11, 2017.
10. Sharma, J., Optimised design and development of a bio-medical healthcare device through quality function deployment (QFD). *Int. J. Electron. Healthc.* 7(1):68–87, 2012.
11. Arakawa, T., Xie, R., Seshima, F. et al., Air bio-battery with a gas/liquid porous diaphragm cell for medical and health care devices. *Biosens. Bioelectron.* 103:171–175, 2018.
12. Marassi, V., Di, L. C., Smith, S. et al., Silver nanoparticles as a medical device in healthcare settings: a five-step approach for candidate screening of coating agents. *R. Soc. Open Sci.* 5(1):171113, 2018.
13. Chaudhari, K., Ukil, A., Kumar, K. N. et al., Hybrid Optimization for Economic Deployment of ESS in PV-Integrated EV Charging Stations. *IEEE Transactions on Industrial Informatics* 14(1):106–116, 2018.
14. Pevec, D., Babic, J., Kayser, M. A. et al., A data-driven statistical approach for extending electric vehicle charging infrastructure. *Int. J. Energy Res.* 42(4):3102–3120, 2018.
15. Jandak, V., Svec, P., Jiricek, O. et al., Piezoelectric line moment actuator for active radiation control from light-weight structures. *Mech. Syst. Signal Process.* 96:260–272, 2017.
16. Malyshevsky, V. S., and Fomin, G. V., Electromagnetic Radiation in the Atmosphere Generated by Excess Negative Charge in a Nuclear-Electromagnetic Cascade. *Russ. Phys. J.* 59(9):1–6, 2017.
17. Sambo, Y. A., Héliot, F., and Imran, M. A., A Survey and Tutorial of Electromagnetic Radiation and Reduction in Mobile Communication Systems. *IEEE Communications Surveys & Tutorials* 17(2):790–802, 2017.
18. YU, S. et al., *Case Analysis and Application of MATLAB Optimized Algorithms (Advanced Version)*. Beijing: Tsinghua University Press, 2015.

Publisher's Note Springer Nature remains neutral with regard to jurisdictional claims in published maps and institutional affiliations.

Reproduced with permission of copyright owner. Further reproduction prohibited without permission.